












TECH BRIEFS

NATIONAL AERONAUTICS AND SPACE ADMINISTRATION

-  **Technology Focus**
-  **Computers/Electronics**
-  **Software**
-  **Materials**
-  **Mechanics**
-  **Machinery/Automation**
-  **Manufacturing**
-  **Bio-Medical**
-  **Physical Sciences**
-  **Information Sciences**
-  **Books and Reports**

INTRODUCTION

Tech Briefs are short announcements of innovations originating from research and development activities of the National Aeronautics and Space Administration. They emphasize information considered likely to be transferable across industrial, regional, or disciplinary lines and are issued to encourage commercial application.

Availability of NASA Tech Briefs and TSPs

Requests for individual Tech Briefs or for Technical Support Packages (TSPs) announced herein should be addressed to

National Technology Transfer Center

Telephone No. (800) 678-6882 or via World Wide Web at www2.nttc.edu/leads/

Please reference the control numbers appearing at the end of each Tech Brief. Information on NASA's Innovative Partnerships Program (IPP), its documents, and services is also available at the same facility or on the World Wide Web at <http://ipp.nasa.gov>.

Innovative Partnerships Offices are located at NASA field centers to provide technology-transfer access to industrial users. Inquiries can be made by contacting NASA field centers and Mission Directorates listed below.

NASA Field Centers and Program Offices

Ames Research Center

Lisa L. Lockyer
(650) 604-1754
lisa.l.lockyer@nasa.gov

Dryden Flight Research Center

Gregory Poteat
(661) 276-3872
greg.poteat@dfrc.nasa.gov

Goddard Space Flight Center

Nona Cheeks
(301) 286-5810
Nona.K.Cheeks.1@nasa.gov

Jet Propulsion Laboratory

Ken Wolfenbarger
(818) 354-3821
james.k.wolfenbarger@jpl.nasa.gov

Johnson Space Center

Helen Lane
(713) 483-7165
helen.w.lane@nasa.gov

Kennedy Space Center

Jim Aliberti
(321) 867-6224
Jim.Aliberti-1@nasa.gov

Langley Research Center

Ray P. Turcotte
(757) 864-8881
r.p.turcotte@larc.nasa.gov

John H. Glenn Research Center at Lewis Field

Robert Lawrence
(216) 433-2921
robert.f.lawrence@nasa.gov

Marshall Space Flight Center

Vernotto McMillan
(256) 544-2615
vernotto.mcmillan@msfc.nasa.gov

Stennis Space Center

John Bailey
(228) 688-1660
john.w.bailey@nasa.gov

NASA Mission Directorates

At NASA Headquarters there are four Mission Directorates under which there are seven major program offices that develop and oversee technology projects of potential interest to industry:

Carl Ray

Small Business Innovation
Research Program (SBIR) &
Small Business Technology
Transfer Program (STTR)
(202) 358-4652
carl.g.ray@nasa.gov

Frank Schowengerdt

Innovative Partnerships Program
(Code TD)
(202) 358-2560
fschowen@hq.nasa.gov

John Mankins

Exploration Systems Research
and Technology Division
(202) 358-4659
john.c.mankins@nasa.gov

Terry Hertz

Aeronautics and Space Mission
Directorate
(202) 358-4636
thertz@mail.hq.nasa.gov

Glen Mucklow

Mission and Systems
Management Division (SMD)
(202) 358-2235
gmucklow@mail.hq.nasa.gov

Granville Paules

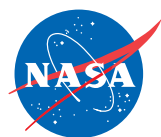
Mission and Systems
Management Division (SMD)
(202) 358-0706
gpaules@mtpe.hq.nasa.gov

Gene Trinh

Human Systems Research and
Technology Division (ESMD)
(202) 358-1490
eugene.h.trinh@nasa.gov

John Rush

Space Communications Office
(SOMD)
(202) 358-4819
john.j.rush@nasa.gov



TECH BRIEFS

NATIONAL AERONAUTICS AND SPACE ADMINISTRATION



5 Technology Focus: Test & Measurement

- 5 Laser System for Precise, Unambiguous Range Measurements
- 6 Flexible Cryogenic Temperature and Liquid-Level Probes
- 7 Precision Cryogenic Dilatometer
- 8 Stroboscopic Interferometer for Measuring Mirror Vibrations



9 Electronics/Computers

- 9 Some Improvements in H-PDLCs
- 9 Multiple-Bit Differential Detection of OQPSK
- 10 Absolute Position Encoders With Vertical Image Binning
- 11 Flexible, Carbon-Based Ohmic Contacts for Organic Transistors
- 12 GaAs QWIP Array Containing More Than a Million Pixels



13 Software

- 13 AutoChem
- 13 Virtual Machine Language
- 13 Two-Dimensional Ffowcs Williams/Hawkings Equation Solver
- 13 Full Multigrid Flow Solver
- 14 Doclet To Synthesize UML
- 14 Computing Thermal Effects of Cavitation in Cryogenic Liquids
- 14 GUI for Computational Simulation of a Propellant Mixer
- 14 Control Program for an Optical-Calibration Robot
- 14 SQL-RAMS
- 15 Distributing Data From Desktop to Hand-Held Computers
- 15 Best-Fit Conic Approximation of Spacecraft Trajectory



17 Materials

- 17 Improved Charge-Transfer Fluorescent Dyes



19 Mechanics

- 19 Stability-Augmentation Devices for Miniature Aircraft
- 19 Tool Measures Depths of Defects on a Case Tang Joint



21 Manufacturing

- 21 Two Heat-Transfer Improvements for Gas Liquefiers
- 21 Controlling Force and Depth in Friction Stir Welding



23 Physical Sciences

- 23 Spill-Resistant Alkali-Metal-Vapor Dispenser
- 23 A Methodology for Quantifying Certain Design Requirements During the Design Phase
- 24 Measuring Two Key Parameters of H3 Color Centers in Diamond



27 Information Sciences

- 27 Improved Compression of Wavelet-Transformed Images
- 27 NASA Interactive Forms Type Interface — NIFTI
- 28 Predicting Numbers of Problems in Development of Software



29 Books & Reports

- 29 Hot-Electron Photon Counters for Detecting Terahertz Photons
- 29 Magnetic Variations Associated With Solar Flares
- 29 Artificial Intelligence for Controlling Robotic Aircraft

This document was prepared under the sponsorship of the National Aeronautics and Space Administration. Neither the United States Government nor any person acting on behalf of the United States Government assumes any liability resulting from the use of the information contained in this document, or warrants that such use will be free from privately owned rights.



Laser System for Precise, Unambiguous Range Measurements

Simultaneous, overlapping, coarse-resolution measurements would resolve ambiguities in fine-resolution measurements.

NASA's Jet Propulsion Laboratory, Pasadena, California

The **Modulation Sideband Technology for Absolute Range (MSTAR)** architecture is the basis of design of a proposed laser-based heterodyne interferometer that could measure a range (distance) as great as 100 km with a precision and resolution of the order of 1 nm. Simple optical interferometers can measure changes in range with nanometer resolution, but cannot measure range itself because interference is subject to the well-known integer-multiple-of- 2π -radians phase ambiguity, which amounts to a range ambiguity of the order of 1 μm at typical laser wavelengths. Existing rangefinders have a resolution of the order of 10 μm and are therefore unable to resolve the ambiguity. The proposed MSTAR architecture bridges the gap, enabling nanometer resolution with an ambiguity range that can be extended to arbitrarily large distances.

The MSTAR architecture combines the principle of the heterodyne interferometer with the principle of extending the ambiguity range of an interferometer by using light of two wavelengths. The use of two wavelengths for this purpose is well established in optical metrology, radar, and sonar. However, unlike in traditional two-color laser interferometry, light of two wavelengths would not be generated by two lasers. Instead, multiple wavelengths would be generated as sidebands of phase modulation of the light from a single frequency-stabilized laser. The phase modulation would be effected by applying sinusoidal signals of suitable frequencies (typically tens of gigahertz) to high-speed electro-optical phase modulators. Intensity modulation can also be used.

An MSTAR system (see figure) would include a conventional laser heterodyne interferometer as a subsystem, plus two

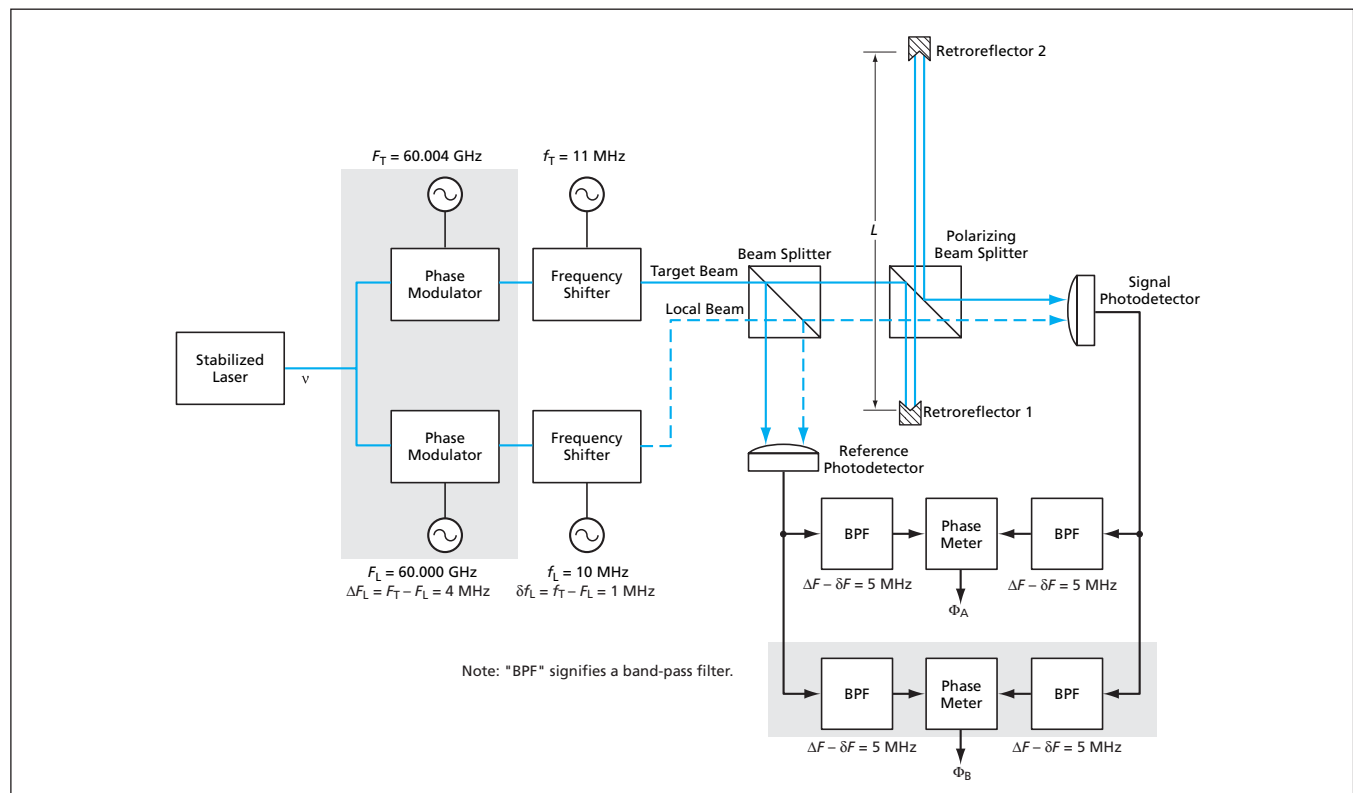
high-speed phase modulators and a second phase meter. The light from the laser of carrier frequency ν would first be split into a target beam and a local beam. The target beam would be phase-modulated by a sinusoid of frequency F_T , producing sidebands displaced from the laser (carrier) frequency at positive and negative integer multiples of F_T . The carrier and all the sidebands would then be shifted in frequency by f_T . The local beam would be processed similarly, except that it would be phase-modulated at a frequency F_L and shifted in frequency by f_L . The corresponding frequencies are chosen to differ from each other by convenient small amounts:

$$\Delta F = F_T - F_L$$

and

$$\delta f = f_T - f_L$$

The primary innovation of the MSTAR architecture is the selection of



An **MSTAR System** would include a conventional heterodyne laser interferometer plus the additional components depicted in the shaded areas. This system would provide phase measurements Φ_A and Φ_B that, taken together with a coarse range measurement by a pulsed ranging sensor, would yield an unambiguous measure of length L to high resolution.

phase-modulation and shift frequencies such that every sideband order m forms a heterodyne pair with a distinct heterodyne frequency,

$$m\Delta F - \delta f.$$

The signal from each heterodyne pair can be isolated by appropriate filtering. In the case illustrated in the figure, one would choose the first upper sideband pair ($m = +1$) and the first lower sideband pair ($m = -1$). Filters would isolate heterodyne frequencies

$$\begin{aligned} f_A &= \Delta F + \delta f \\ \text{and} \\ f_B &= \Delta F - \delta f. \end{aligned}$$

The phase-meter outputs would be

$$\phi_A = 2\pi(v + f_T + F_T)2L/c$$

and

$$\phi_B = 2\pi(v + f_T - F_T)2L/c,$$

where L is the distance that one seeks to measure and c is the speed of light. Each of these outputs would be characterized by the same range resolution and ambiguity range as those of a conventional heterodyne interferometer, and, as such, would constitute the fine incremental range outputs. The difference between these outputs,

$$\phi_A - \phi_B = 8\pi F_T L/c$$

would constitute the gap-bridging coarse incremental range output, char-

acterized by an ambiguity range of $c/4F_T$. One could lower the modulation frequency, F_T , to extend the ambiguity range as needed.

This work was done by Serge Dubovitsky and Oliver Lay of Caltech for NASA's Jet Propulsion Laboratory. Further information is contained in a TSP (see page 1).

This invention is owned by NASA, and a patent application has been filed. Inquiries concerning nonexclusive or exclusive license for its commercial development should be addressed to the Patent Counsel, NASA Management Office-JPL (818) 354-7770. Refer to NPO-30304.

Flexible Cryogenic Temperature and Liquid-Level Probes

These probes can be readily customized.

Stennis Space Center, Mississippi

Lightweight, flexible probes have been developed for measuring temperatures at multiple locations in tanks that contain possibly pressurized cryogenic fluids. If the fluid in a given tank is subcritical (that is, if it consists of a liquid and its vapor), then in one of two modes of operation, the temperature measurements made by a probe of this type can be used to deduce the approximate level of the liquid.

The temperature sensors are silicon diodes located at intervals along a probe. If the probe is to be used to measure a temperature gradient along a given axis in the tank, then the probe must be mounted along that axis. In the temperature-measurement mode, a constant small electric current is applied to each diode and the voltage

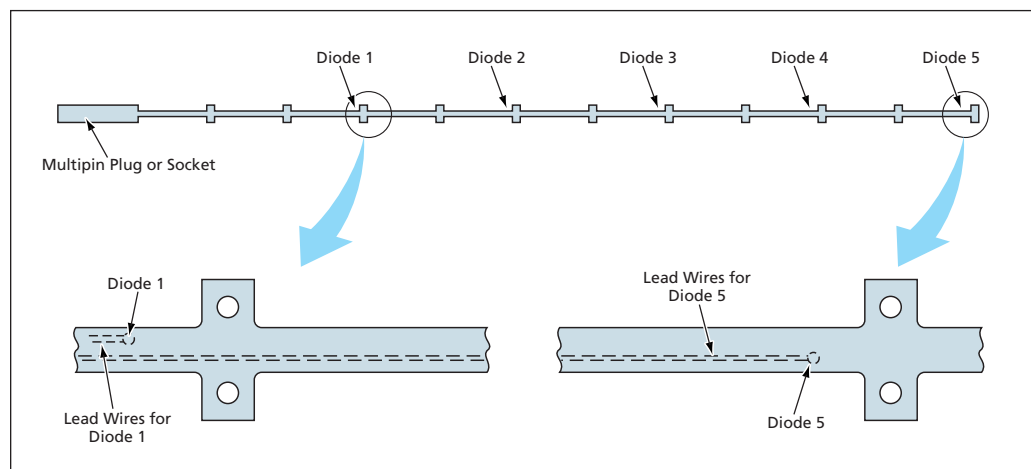
across the diode — a known function of the current and temperature — is measured as an indication of its temperature. For the purpose of this measurement, "small electric current" signifies a current that is not large enough to cause a significant increase in the measured temperature. More specifically, the probe design calls for a current of 10 μA , which, in the cryogenic temperature range of interest, generates heat at a rate of only about 0.01 mW per diode.

In the liquid-level-sensing mode, one applies a larger current (30 mA) to each diode so as to heat each diode appreciably (with a power of about 36 mW in the temperature range of interest). Because the liquid cools the diode faster than does the

vapor, the temperature of the diode is less when the diode is immersed in the liquid than when it is above the surface of the liquid. Thus, the temperature (voltage) reading from each diode can be used to determine whether the liquid level is above or below the diode, and one can deduce that the liquid level lies between two adjacent diodes, the lower one of which reads a significantly lower temperature.

The aforementioned techniques for measuring temperature and deducing liquid level are not new. What is new here are the designs of the probes and of associated external electronic circuitry. In each probe, the diodes and the lead wires are embedded in a strong, lightweight, flexible polyimide

strip. Each probe is constructed as an integral unit that includes a multipin input/output plug or socket for solderless connection of the lead wires to the external circuitry. The polyimide strip includes mounting tabs with holes that can accommodate rivets, screws, or other fasteners. Alternatively, a probe can be mounted by use of an epoxy. A probe can be manufactured to almost any length or width, and the diodes can be embedded at almost any desired



Diodes and Their Lead Wires are embedded in a polyimide strip at locations from which temperature measurements are desired.

location along and across the polyimide strip.

In designing a probe for a specific application, one seeks a compromise between (1) minimizing the number of diodes in order to minimize the complexity of input/output connections and external electronic circuitry while (2) using enough diodes to obtain the required precision. Optionally, to minimize spurious heating of the cryogenic

fluid, the external circuitry can be designed to apply power to the probe only during brief measurement intervals. Assuming that the external circuitry is maintained at a steady temperature, a power-on interval of only a few seconds is sufficient to obtain accurate data on temperatures and/or the height of the liquid/vapor interface.

This work was done by Mark Habersbusch of Sierra Lobo, Inc., for Stennis Space Center.

In accordance with Public Law 96-517, the contractor has elected to retain title to this invention. Inquiries concerning rights for its commercial use should be addressed to:

*Sierra Lobo, Inc.
11401 Hoover Road
Milan, Ohio 44846*

Refer to SSC-00191, volume and number of this NASA Tech Briefs issue, and the page number.

Precision Cryogenic Dilatometer

This instrument offers much greater precision than do other currently available dilatometers.

NASA's Jet Propulsion Laboratory, Pasadena, California

A dilatometer based on a laser interferometer is being developed to measure mechanical creep and coefficients of thermal expansion (CTEs) of materials at temperatures ranging from ambient down to 15 K. This cryogenic dilatometer has been designed to minimize systematic errors that limit the best previously available dilatometers. At its prototype stage of development, this cryogenic dilatometer yields a strain measurement error of 35 ppb or 1.7 ppb/K CTE measurement error for a 20-K thermal load, for low-expansion materials in the temperature range from 310 down to 30 K. Planned further design refinements that include a provision for stabilization of the laser and ad-

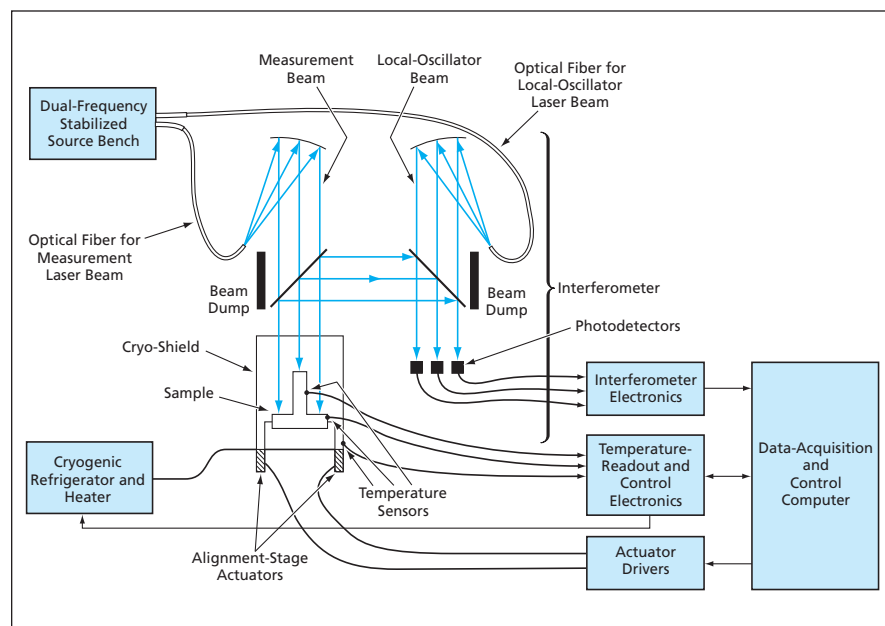
dition of a high-precision sample-holding jig are expected to reduce the measurement error to 5-ppb strain error or 0.3-ppb/K CTE error for a 20-K thermal load.

The dilatometer (see figure) includes a common-path, differential, heterodyne interferometer; a dual-frequency, stabilized source bench that serves as the light source for the interferometer; a cryogenic chamber in which one places the material sample to be studied; a cryogenic system for cooling the interior of the chamber to the measurement temperature; an ultra-stable alignment stage for positioning the chamber so that the sample is properly positioned with respect to

the interferometer; and a data-acquisition and control system. The cryogenic chamber and the interferometer portion of the dilatometer are housed in a vacuum chamber on top of a vibration-isolating optical table in a cleanroom. The sample consists of two pieces — a pillar on a base — both made of the same material. Using reflections of the interferometer beams from the base and the top of the pillar, what is measured is the change in length of the pillar as the temperature in the chamber is changed.

In their fundamental optical and electronic principles of operation, the laser light source and the interferometer are similar to those described in "Common-Path Heterodyne Interferometers" (NPO-20786), *NASA Tech Briefs*, Vol. 25, No. 7 (July 2001), page 12a, and "Interferometer for Measuring Displacement to Within 20 pm" (NPO-21221), *NASA Tech Briefs*, Vol. 27, No. 7 (July 2003), page 8a. However, the present designs incorporate a number of special geometric, optical, and mechanical features to minimize optical and thermal-expansion effects that contribute to measurement errors. These features include the use of low-thermal-expansion materials for structural components, kinematic mounting and symmetrical placement of optical components, and several measures taken to minimize spurious reflections of laser beams.

*This work was done by Matthew Dudik, Peter Halverson, Marie Levine-West, Martin Marcin, Robert D. Peters, and Stuart Shaklan of Caltech for NASA's Jet Propulsion Laboratory. Further information is contained in a TSP (see page 1).
NPO-40389*



The **Change in Height** of the sample pillar in the cryogenic chamber is measured interferometrically. Design features that are much too numerous to depict here ensure a high degree of optical and mechanical stability over wide temperature range, as needed for high-precision measurements of thermal expansion and creep in the sample.

Stroboscopic Interferometer for Measuring Mirror Vibrations

Interferometric snapshots are taken at intervals over a cycle for each vibrational mode.

Marshall Space Flight Center, Alabama

Stroboscopic interferometry is a technique for measuring the modes of vibration of mirrors that are lightweight and, therefore, unavoidably flexible. The technique was conceived especially for modal characterization of lightweight focusing mirror segments to be deployed in outer space; however, the technique can be applied to lightweight mirrors designed for use on Earth as well as the modal investigation of other optical and mechanical structures.

To determine the modal structure of vibration of a mirror, it is necessary to excite the mirror by applying a force that varies periodically with time at a controllable frequency. The excitation can utilize sinusoidal, square, triangular, or even asynchronous waveforms. Because vibrational modes occur at specific resonant frequencies, it is necessary to perform synchronous measurements and sweep the frequency to locate the significant resonant modes. For a given mode it is possible to step the phase of data acquisition in order to capture the modal behavior over a single cycle of the resonant frequency.

In order to measure interferometrically the vibrational response of the mirror at a given frequency, an interfer-

ometer must be suitably aligned with the mirror and adjustably phase-locked with the excitation signal. As in conventional stroboscopic photography, the basic idea in stroboscopic interferometry is to capture an image of the shape of a moving object (in this case, the vibrating mirror) at a specified instant of time in the vibration cycle. Adjusting the phase difference over a full cycle causes the interference fringes to vary over the full range of motion for the mode at the excitation frequency. The interference-fringe pattern is recorded as a function of the phase difference, and, from the resulting data, the surface shape of the mirror for the given mode is extracted.

In addition to the interferometer and the mirror to be tested, the equipment needed for stroboscopic interferometry includes an arbitrary-function generator (that is, a signal generator), an oscilloscope, a trigger filter, and an advanced charge-coupled-device (CCD) camera. The optical components are positioned to form a pupil image of the mirror under test on the CCD chip, so that the interference pattern representative of the instantaneous mirror shape is imaged on the CCD chip.

The mirror is acoustically excited into vibration by use of a loudspeaker or other suitable mechanical transducer. The signal generator provides the sinusoidal signal for driving the loudspeaker. The signal-generator output is also processed through phase-locking and phase-shifting circuitry to generate an adjustably-phase-shifted trigger signal, locked in phase to the excitation signal, for triggering the CCD camera to capture an image at the desired instant during the vibration cycle.

Advanced single-frame phase-shifting interferometers can be used for data acquisition to produce high spatial resolution measurements and "phase movies" of the vibrating surface. The maximum resonant frequency measurable is determined by the camera exposure time for synchronous measurements and camera frame rate for asynchronous excitation. Synchronous measurements at rates up to 100 kHz are possible with this technique.

This work was done by H. Philip Stahl of Marshall Space Flight Center and Ted Rogers of the University of Alabama in Huntsville. Further information is contained in a TSP (see page 1). MFS-32057



Some Improvements in H-PDLCs

Nonuniformities and required drive potentials have been reduced.

Goddard Space Flight Center, Greenbelt, Maryland

Some improvements have been made in the formulation of holographically formed polymer-dispersed liquid crystals (H-PDLCs) and in the fabrication of devices made from these materials, with resulting improvements in performance. H-PDLCs are essentially volume Bragg gratings. Devices made from H-PDLCs function as electrically switchable reflective filters. Heretofore, it has been necessary to apply undesirably high drive voltages in order to switch H-PDLC devices.

Many scientific papers on H-PDLCs and on the potential utility of H-PDLC devices for display and telecommunication applications have been published. However, until now, little has been published about improving quality control in synthesis of H-PDLCs and fabrication of H-PDLC devices to minimize (1) spatial nonuniformities within individual devices, (2) nonuniformities among nominally identical devices, and (3) variations in performance among nominally identical devices. The improvements reported here are results of a research effort directed partly toward solving these quality-control problems and partly toward reducing switching voltages.

The quality-control improvements include incorporation of a number of process controls to create a relatively robust process, such that the H-PDLC devices fabricated in this process are more nearly uniform than were those fabricated in a prior laboratory-type process. The improved process includes ultrasonic mixing, ultrasonic cleaning, the use of a micro dispensing technique, and the use of a bubble press.

The ultrasonic mixing (in contradistinction to other types of mixing) creates more nearly uniform H-PDLCs. The ultrasonic cleaning removes chips of indium tin oxide (which is electrically conductive), whereas, heretofore, chips of indium oxide remaining at the edges of H-PDLC devices have caused electrical short circuits. The micro-dispensing technique enables the emplacement of precisely the amount of H-PDLC required for a given cell volume so that the H-PDLC can be pressed between glass substrates to a precise inter-substrate distance defined by spacers. The bubble press enables the application of the correct pressure needed to push the substrates against the H-PDLC and the controlled

amounts of spacers, thereby also helping to minimize nonuniformity of gaps among cells.

The drive-voltage problem has been partially solved by development of a formulation that includes an additive that reduces the magnitude of the required drive voltage. Devices that can be switched from a reflectivity of ≈ 0.5 to a reflectivity near zero by applying relatively low drive potentials (<100 V) have been demonstrated. It has been postulated that the reduction in the magnitude of the required drive voltage is attributable to a reduction in the surface anchoring energy.

In cases of fabrication of multilayer devices comprising stacked H-PDLC panels, the improved process also includes the use of thin glass substrates with appropriate optical coatings. Devices comprising, variously, five or ten stacked panels have been fabricated thus far.

This work was done by Gregory P. Crawford and Liuliu Li of Brown University for Goddard Space Flight Center. Further information is contained in a TSP (see page 1). GSC-14920-1

Multiple-Bit Differential Detection of OQPSK

This could be the best-known differential-detection method for OQPSK.

NASA's Jet Propulsion Laboratory, Pasadena, California

A multiple-bit differential-detection method has been proposed for the reception of radio signals modulated with offset quadrature phase-shift keying (offset QPSK or OQPSK). The method is also applicable to other spectrally efficient offset quadrature modulations.

This method is based partly on the same principles as those of a multiple-symbol differential-detection method for *M*-ary QPSK, which includes QPSK (that is, non-offset QPSK) as a special case. That method was introduced more

than a decade ago by the author of the present method as a means of improving performance relative to a traditional (two-symbol observation) differential-detection scheme. Instead of symbol-by-symbol detection, both that method and the present one are based on a concept of maximum-likelihood sequence estimation (MLSE). As applied to the modulations in question, MLSE involves consideration of (1) all possible binary data sequences that could have been received during an observation time of some number, N , of symbol periods and

(2) selection of the sequence that yields the best match to the noise-corrupted signal received during that time. The performance of the prior method was shown to range from that of traditional differential detection for short observation times (small N) to that of ideal coherent detection (with differential encoding) for long observation times (large N).

The mathematical derivation of the present method began with the identification of an equivalent precoded continuous phase modulation (CPM)

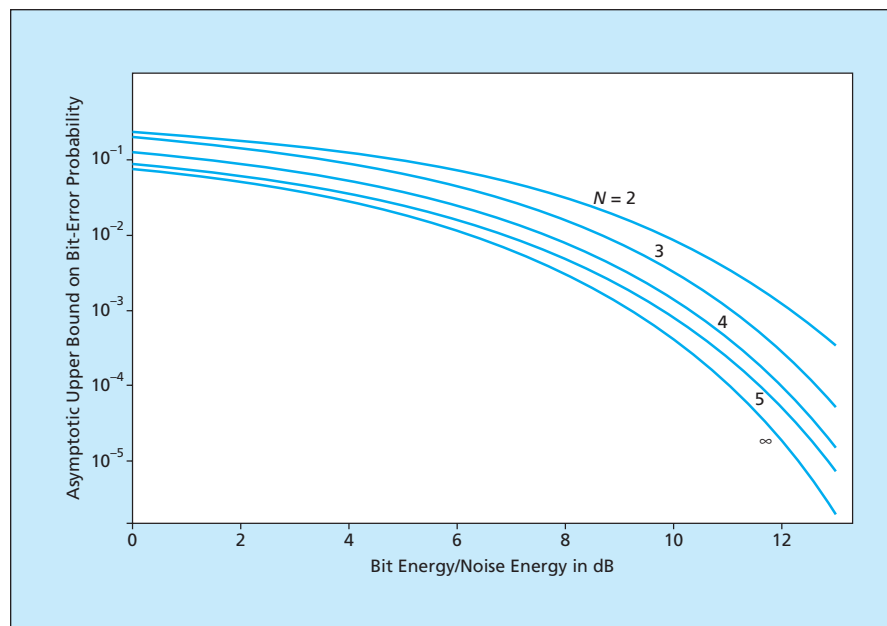
structure, first for OQPSK and then differentially encoded OQPSK. It was shown that the precoding needed to

obtain the equivalence is such as to result in a ternary (0,-1,+1) CPM input alphabet that, during any given one-bit

observation period, is equivalent to a binary alphabet. Next, some results of prior work by the same author on maximum-likelihood block detection of noncoherent CPM were utilized to derive a maximum-likelihood decision metric and an associated receiver structure for the precoded version that equivalently represents differentially encoded OQPSK.

The figure presents some results of computations of the bit-error performance of the present method. Because of its maximum-likelihood basis, this method is expected to be the most power-efficient method of differential detection of OQPSK. Furthermore, on the basis of the resemblance of this method to the prior multiple-symbol method of differential detection of non-offset QPSK, the performance of a receiver based on this method is expected to improve with increasing N .

*This work was done by Marvin Simon of Caltech for NASA's Jet Propulsion Laboratory. Further information is contained in a TSP (see page 1).
NPO-30777*



The **Asymptotic Upper Bound on the Average Bit-Error Probability** for a receiver based on the proposed method has been computed as a function of the bit-energy/noise-energy ratio and the number (N) of bit periods in the observation time.

Absolute Position Encoders With Vertical Image Binning

Conversion rates can exceed 20 kHz.

Goddard Space Flight Center, Greenbelt, Maryland

Improved optoelectronic pattern-recognition encoders that measure rotary and linear 1-dimensional positions at conversion rates (numbers of readings per unit time) exceeding 20 kHz have been invented. Heretofore, optoelectronic pattern-recognition absolute-position encoders have been limited to conversion rates <15 Hz — too low for emerging industrial applications in which conversion rates ranging from 1 kHz to as much as 100 kHz are required. The high conversion rates of the improved encoders are made possible, in part, by use of vertically compressible or binnable (as described below) scale patterns in combination with modified readout sequences of the image sensors [charge-coupled devices (CCDs)] used to read the scale patterns. The modified readout sequences and the processing of the images thus read out are amenable to implementation by use of modern, high-speed, ultra-compact microprocessors and digital signal processors or field-programmable gate arrays. This combination of improvements makes it

possible to greatly increase conversion rates through substantial reductions in all three components of conversion time: exposure time, image-readout time, and image-processing time.

In a typical prior optoelectronic pattern-recognition absolute-position encoder, the CCD is oriented with its horizontal axis parallel to the axis along

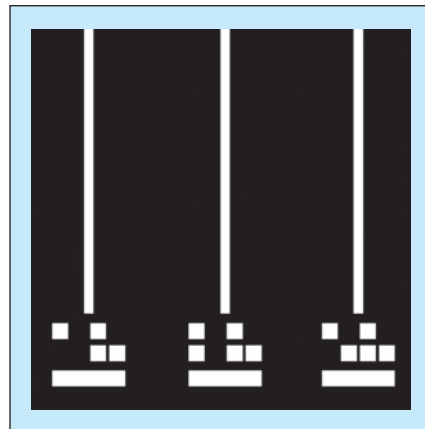


Figure 1. **Previous Patterns Contain Both Vertical and Horizontal Information** and must be read out pixel-by-pixel.

which the position of the scale pattern is to be measured. The pattern includes vertically oriented fiducial bars plus small rectangles or squares, representing code bits, that serve to uniquely identify the fiducial bars (see Figure 1). The lower limit on conversion time is determined primarily by the exposure time and the time required to read out the

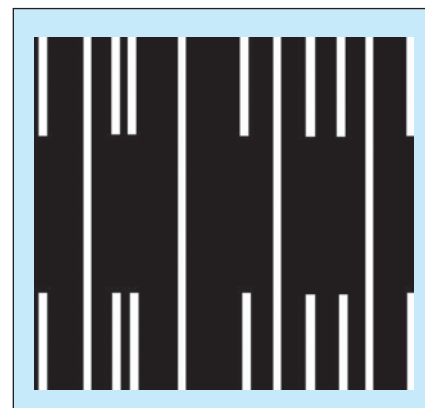


Figure 2. **Portion of New Scale Pattern**, partly resembling common bar code, is representative of vertically binnable patterns used in encoders of the type described in the text.

entire image from the CCD, pixel by pixel. The exposure time must be long enough to obtain adequate signal-to-noise ratios in the code-bit marks. The requirement for pixel-by-pixel readout of the entire image arises from the use of vertical (as well as horizontal) position information to distinguish among code-bit marks in different rows.

In conventional pixel-by-pixel readout, during each row-readout clock cycle, the signal contents of all the pixels of each row are shifted down to the next row, except that the contents of the bottom row are shifted down to a serial register, which triggers analog-to-digital conversion of each pixel's signal. Then, before the beginning of the next row-readout clock cycle, the contents of the serial register are shifted out, one pixel at a time, in response to sequence of column-readout pulses.

In vertically binned readout, which is an established alternative to conventional pixel-by-pixel readout, the sequence of clock pulses is modified so that the contents of multiple rows are shifted down to the serial register before applying the column-readout

pulses. As a result, vertical resolution is lost, but time needed for reading out the image charge from all the pixels is reduced by a factor equal to the number of rows shifted prior to shifting the column contents out of the serial register. Moreover, the image-data processes needed to extract the vertical spatial information to determine row locations of code-bit marks can be eliminated. Inasmuch as the consequent loss of vertical resolution does not adversely affect the desired measurement of horizontal position, vertical binning can thus be used to reduce readout time substantially, provided that the scale pattern is such that the horizontal spatial information in the code-bit marks suffices to uniquely identify the fiducial bars. A scale pattern that satisfies this requirement is said to be vertically binnable.

Figure 2 shows an example of a vertically binnable scale pattern. The vertical stripes spanning the entire field from top to bottom are the fiducial bars. The stripes that extend part way up from the bottom and part way down from the top are the code-bit marks. The code-bit

marks at the top and bottom are identical, so that the image can be binned by the full height (that is, all the rows can be included in the bin for each column, enabling maximum speedup). Other patterns in which code bits at top and bottom differ but identify a greater number of fiducials dramatically increase range, while still greatly speeding up readout. Among the secondary advantages of such a vertically binnable pattern is that the vertical alignment of the CCD relative to the pattern is much less critical than is the alignment needed to utilize the vertical spatial information in a conventional pattern with pixel-by-pixel readout.

This work was done by Douglas B. Leviton of Goddard Space Flight Center. Further information is contained in a TSP (see page 1).

This invention is owned by NASA, and a patent application has been filed. Inquiries concerning nonexclusive or exclusive license for its commercial development should be addressed to the Patent Counsel, Goddard Space Flight Center, (301) 286-7351. Refer to GSC-14633-1.

Flexible, Carbon-Based Ohmic Contacts for Organic Transistors

These contacts are printed using an inexpensive, low-temperature process.

NASA's Jet Propulsion Laboratory, Pasadena, California

A low-temperature process for fabricating flexible, ohmic contacts for use in organic thin-film transistors (OTFTs) has been developed. Typical drain-source contact materials used previously for OTFTs include (1) vacuum-deposited noble-metal contacts and (2) solution-deposited intrinsically conducting molecular or polymeric contacts. Both of these approaches, however, have serious drawbacks.

Use of vacuum-deposited noble-metal contacts (such as gold or platinum) obviates one of the main benefits of organic electronics, which is low-cost processing based on solution or printing techniques. First, it requires the use of vacuum-deposition techniques (such as sputtering or evaporation) instead of the less expensive solution-based processes such as spin coating, casting, or printing. Second, the use of gold or platinum for coating large-area devices is potentially expensive (both from a standpoint of materials and processing equipment). Again, this approach runs counter to the perceived low-cost benefit of organic

electronics. Furthermore, adhesion of gold to many organic materials is very poor. Some recent work has been carried out regarding intrinsically conducting molecular- or polymeric-based contacts such as polyaniline and TTF-TCNQ. Unfortunately, these materials tend to exhibit high resistivities and poor overall performance, are prone to reaction with the surrounding environment, and are potentially unstable with time.

To achieve an ohmic contact to the organic semiconductor, the work function of the contact should be well matched to that of the semiconductor. Due to the similar chemical nature of the graphite filler to the conjugated poly(3-hexylthiophene) (P3HT) polymer, it was surmised that a carbon paste may possess a similar work function and therefore behave as suitable ohmic contact in this application.

To demonstrate the effectiveness of this approach, bottom contact thin-film transistors were fabricated (Fig. 1). A highly doped silicon wafer was

used as the substrate, with a thermally grown 300-nm oxide gate dielectric layer. In this case, a 5-mil (127- μ m) thick laser-cut stainless-steel stencil was used to pattern the contacts.

The carbon-based conductor used was a paste comprising a stable, flexible polymer binder and a conducting graphite/carbon-based filler. The

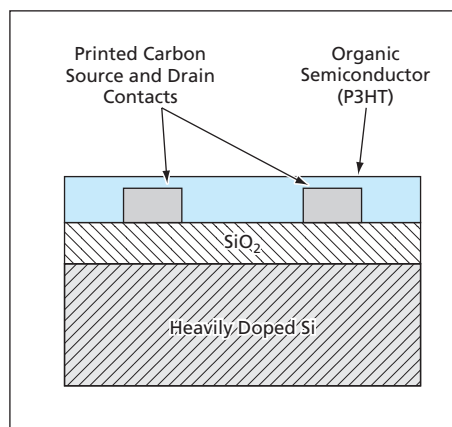


Figure 1. An **Organic Field-Effect Transistor** was fabricated in an inexpensive process, mostly at room temperature, with brief heating at 100 °C.

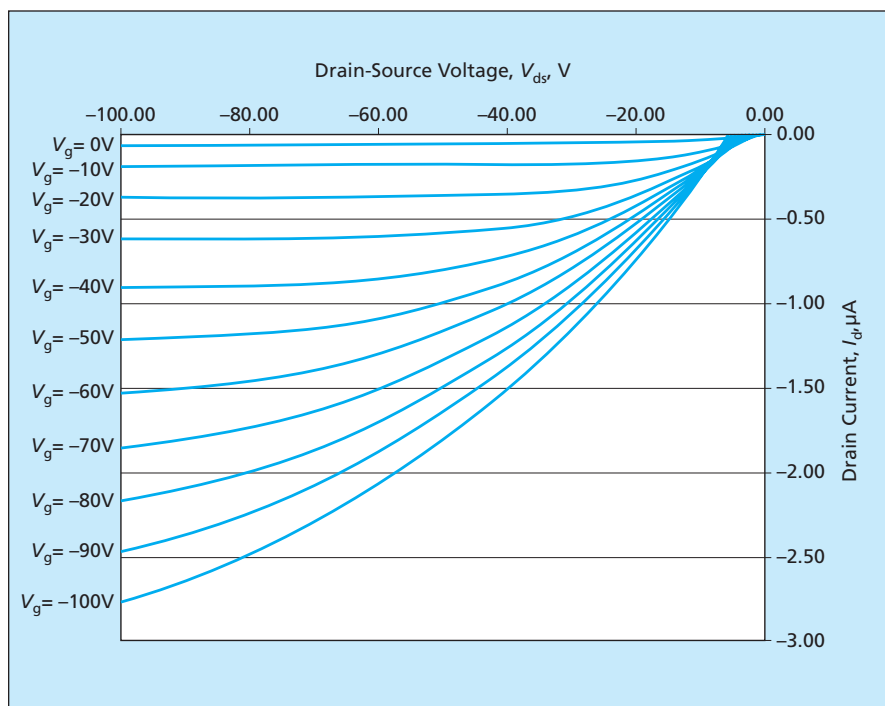


Figure 2. These **Current-Versus-Voltage Curves**, obtained from measurements on a device like that of Figure 1, are characteristic of a field-effect transistor.

paste was stencil-printed through the apertures using a metal squeegee, and the contacts were cured at 100 °C on a hot plate for 30 minutes. The P3HT material was then drop cast on the surface of the substrate, over the printed contacts. Contact was made to the cleaved wafer to form the gate. Contact was made to the drain and source carbon contacts through

probes connected to micromanipulators. Device measurements were conducted on an HP 4145B semiconductor parameter analyzer, with the drain-source voltage varying from 0 to -100 V, and the gate bias varying from 0 to -100 V in -10 V steps.

As seen in Fig. 2, very good transistor curves are obtained from the devices, indicating clear field-effect phenomena,

which demonstrates the effectiveness of the carbon-based contacts. In this case, a device with a channel length of 500 μm and a channel width of 5,000 μm was measured (multiple devices were characterized to verify repeatability of the data). Other device geometries are possible, as printed feature sizes down to 37 μm have been demonstrated using state-of-the-art thick-film stencil/screen printing techniques.

Enhancement of the drain-source current is clearly seen as a function of increasing gate bias in Fig. 2. In this case, an I_{on}/I_{off} ratio of 44 was determined at $V_{ds} = -100$ V, with $V_g = 0$ (I_{off}) and $V_g = -100$ V (I_{on}). A carrier mobility of $\mu \approx 0.007$ cm²/V-s was also estimated from the data.

This work was done by Erik Brandon of Caltech for NASA's Jet Propulsion Laboratory. Further information is contained in a TSP (see page 1).

In accordance with Public Law 96-517, the contractor has elected to retain title to this invention. Inquiries concerning rights for its commercial use should be addressed to:

*Innovative Technology Assets Management
JPL*

*Mail Stop 202-233
4800 Oak Grove Drive
Pasadena, CA 91109-8099
(818) 354-2240*

E-mail: iaoffice@jpl.nasa.gov

Refer to NPO-40168, volume and number of this NASA Tech Briefs issue, and the page number.

GaAs QWIP Array Containing More Than a Million Pixels

GaAs offers advantages over InSb and HgCdTe.

Goddard Space Flight Center, Greenbelt, Maryland

A 1,024 × 1,024-pixel array of quantum-well infrared photodetectors (QWIPs) has been built on a 1.8 × 1.8-cm GaAs chip. In tests, the array was found to perform well in detecting images at wavelengths from 8 to 9 μm in operation at temperatures between 60 and 70 K. The largest-format QWIP prior array that performed successfully in tests contained 512 × 640 pixels.

There is continuing development effort directed toward satisfying actual and anticipated demands to increase numbers of pixels and pixel sizes in order to increase the imaging resolution of infrared photodetector arrays. A 1,024 × 1,024-pixel and even larger formats have

been achieved in the InSb and HgCdTe material systems, but photodetector arrays in these material systems are very expensive and manufactured by fewer than half a dozen large companies. In contrast, GaAs-photodetector-array technology is very mature, and photodetectors in the GaAs material system can be readily manufactured by a wide range of industrial technologists, by universities, and government laboratories.

There is much similarity between processing in the GaAs industry and processing in the pervasive silicon industry. With respect to yield and cost, the performance of GaAs technology substantially exceeds that of InSb and HgCdTe

technologies. In addition, GaAs detectors can be designed to respond to any portion of the wavelength range from 3 to about 16 μm — a feature that is very desirable for infrared imaging. GaAs QWIP arrays, like the present one, have potential for use as imaging sensors in infrared measuring instruments, infrared medical imaging systems, and infrared cameras.

This work was performed by Murzy Jhabvala of Goddard Space Flight Center and K. K. Choi of the U. S. Army Research Lab and Sarath Gunapala of NASA's Jet Propulsion Laboratory. For further information, contact the Goddard Innovative Partnerships Office at (301) 286-5810. GSC-14688-1

AutoChem

AutoChem is a suite of Fortran 90 computer programs for the modeling of kinetic reaction systems. AutoChem performs automatic code generation, symbolic differentiation, analysis, and documentation. It produces a documented stand-alone system for the modeling and assimilation of atmospheric chemistry. Given databases of chemical reactions and a list of constituents defined by the user, AutoChem automatically does the following:

1. Selects the subset of reactions that involve a user-defined list of constituents and automatically prepares a document listing the reactions;
2. Constructs the ordinary differential equations (ODEs) that describe the reactions as functions of time and prepares a document containing the ODEs;
3. Symbolically differentiates the time derivatives to obtain the Jacobian and prepares a document containing the Jacobian;
4. Symbolically differentiates the Jacobian to obtain the Hessian and prepares a document containing the Hessian; and
5. Writes all the required Fortran 90 code and datafiles for a stand-alone chemical modeling and assimilation system (implementation of steps 1 through 5).

Typically, the time taken for steps 1 through 5 is about 3 seconds. The modeling system includes diagnostic components that automatically analyze each ODE at run time, the relative importance of each term, time scales, and other attributes of the model.

This program was written by David John Lary of Goddard Space Flight Center. Further information is contained in a TSP (see page 1). GSC-14862-1

Virtual Machine Language

Virtual Machine Language (VML) is a mission-independent, reusable software system for programming for spacecraft operations. Features of VML include a rich set of data types, named functions, parameters, IF and WHILE control structures, polymorphism, and on-the-fly creation of spacecraft commands from calculated values. Spacecraft functions can be abstracted into named blocks that re-

side in files aboard the spacecraft. These named blocks accept parameters and execute in a repeatable fashion. The sizes of uplink products are minimized by the ability to call blocks that implement most of the command steps. This block approach also enables some autonomous operations aboard the spacecraft, such as aerobraking, telemetry conditional monitoring, and anomaly response, without developing autonomous flight software. Operators on the ground write blocks and command sequences in a concise, high-level, human-readable programming language (also called "VML"). A compiler translates the human-readable blocks and command sequences into binary files (the operations products). The flight portion of VML interprets the uplinked binary files. The ground subsystem of VML also includes an interactive sequence-execution tool hosted on workstations, which runs sequences at several thousand times real-time speed, affords debugging, and generates reports. This tool enables iterative development of blocks and sequences within times of the order of seconds.

This program was written by Christopher Grasso, Dennis Page, and Taifun O'Reilly with support from Ralph Fleichert, Patricia Lock, Imin Lin, Keith Naviaux, and John Sisino of Caltech for NASA's Jet Propulsion Laboratory. Further information is contained in a TSP (see page 1).

This software is available for commercial licensing. Please contact Karina Edmonds of the California Institute of Technology at (818) 393-2827. Refer to NPO-40365.

Two-Dimensional Ffowcs Williams/Hawkings Equation Solver

FWH2D is a Fortran 90 computer program that solves a two-dimensional (2D) version of the equation, derived by J. E. Ffowcs Williams and D. L. Hawkings, for sound generated by turbulent flow. FWH2D was developed especially for estimating noise generated by airflows around such approximately 2D airframe components as slats. The user provides input data on fluctuations of pressure, density, and velocity on some surface. These data are combined with information about the geometry of the surface to calculate histories of thickness and loading terms. These histories are fast-

Fourier-transformed into the frequency domain. For each frequency of interest and each observer position specified by the user, kernel functions are integrated over the surface by use of the trapezoidal rule to calculate a pressure signal. The resulting frequency-domain signals are inverse-fast-Fourier-transformed back into the time domain. The output of the code consists of the time- and frequency-domain representations of the pressure signals at the observer positions. Because of its approximate nature, FWH2D overpredicts the noise from a finite-length (3D) component. The advantage of FWH2D is that it requires a fraction of the computation time of a 3D Ffowcs Williams/Hawkings solver.

This program was written by David P. Lockard of Langley Research Center. Further information is contained in a TSP (see page 1). LAR-16338-1

Full Multigrid Flow Solver

FMG3D (full multigrid 3 dimensions) is a pilot computer program that solves equations of fluid flow using a finite difference representation on a structured grid. Infrastructure exists for three dimensions but the current implementation treats only two dimensions. Written in Fortran 90, FMG3D takes advantage of the recursive-subroutine feature, dynamic memory allocation, and structured-programming constructs of that language. FMG3D supports multi-block grids with three types of block-to-block interfaces: periodic, C-zero, and C-infinity. For all three types, grid points must match at interfaces. For periodic and C-infinity types, derivatives of grid metrics must be continuous at interfaces. The available equation sets are as follows: scalar elliptic equations, scalar convection equations, and the pressure-Poisson formulation of the Navier-Stokes equations for an incompressible fluid. All the equation sets are implemented with nonzero forcing functions to enable the use of user-specified solutions to assist in verification and validation. The equations are solved with a full multigrid scheme using a full approximation scheme to converge the solution on each succeeding grid level. Restriction to the next coarser mesh uses direct injection for variables and full weighting for residual quantities; prolongation of the coarse grid correction from the coarse

mesh to the fine mesh uses bilinear interpolation; and prolongation of the coarse grid solution uses bicubic interpolation.

*This program was written by Raymond E. Mineck, James L. Thomas, and Robert T. Biedron of Langley Research Center and Boris Diskin of the National Institute of Aerospace. Further information is contained in a TSP (see page 1).
LAR-16608-1*

Doclet To Synthesize UML

The RoseDoclet computer program extends the capability of Java doclet software to automatically synthesize Unified Modeling Language (UML) content from Java language source code. [Doclets are Java-language programs that use the doclet application programming interface (API) to specify the content and format of the output of Javadoc. Javadoc is a program, originally designed to generate API documentation from Java source code, now also useful as an extensible engine for processing Java source code.] RoseDoclet takes advantage of Javadoc comments and tags already in the source code to produce a UML model of that code. RoseDoclet applies the doclet API to create a doclet passed to Javadoc. The Javadoc engine applies the doclet to the source code, emitting the output format specified by the doclet. RoseDoclet emits a Rose model file and populates it with fully documented packages, classes, methods, variables, and class diagrams identified in the source code. The way in which UML models are generated can be controlled by use of new Javadoc comment tags that RoseDoclet provides. The advantage of using RoseDoclet is that Javadoc documentation becomes leveraged for two purposes: documenting the as-built API and keeping the design documentation up to date.

*This program was written by Matthew R. Barry and Richard N. Osborne of United Space Alliance for Johnson Space Center. For further information, contact the Johnson Technology Transfer Office at (281) 483-3809.
MSC-23580*

Computing Thermal Effects of Cavitation in Cryogenic Liquids

A computer program implements a numerical model of thermal effects of cavitation in cryogenic fluids. The

model and program were developed for use in designing and predicting the performances of turbopumps for cryogenic fluids. Prior numerical models used for this purpose do not account for either the variability of properties of cryogenic fluids or the thermal effects (especially, evaporative cooling) involved in cavitation. It is important to account for both because in a cryogenic fluid, the thermal effects of cavitation are substantial, and the cavitation characteristics are altered by coupling between the variable fluid properties and the phase changes involved in cavitation. The present model accounts for both thermal effects and variability of properties by incorporating a generalized representation of the properties of cryogenic fluids into a generalized compressible-fluid formulation for a cavitating pump. The model has been extensively validated for liquid nitrogen and liquid hydrogen. Using the available data on the properties of these fluids, the model has been shown to predict accurate temperature-depression values.

*This program was written by Ashvin Hosangadi, Vineet Ahuja, and Sanford M. Dash of Combustion Research and Flow Technology, Inc., for Marshall Space Flight Center. For further information, contact Ashvin Hosangadi at hosangad@craft-tech.com.
MFS-32140*

GUI for Computational Simulation of a Propellant Mixer

Control Panel is a computer program that generates a graphical user interface (GUI) for computational simulation of a rocket-test-stand propellant mixer in which gaseous hydrogen (GH₂) is injected into flowing liquid hydrogen (LH₂) to obtain a combined flow having desired thermodynamic properties. The GUI is used in conjunction with software that models the mixer as a system having three inputs (the positions of the GH₂ and LH₂ inlet valves and an outlet valve) and three outputs (the pressure inside the mixer and the outlet flow temperature and flow rate). The user can specify valve characteristics and thermodynamic properties of the input fluids via user-friendly dialog boxes. The user can enter temporally varying input values or temporally varying desired output values. The GUI provides (1) a set-point calculator function for determining fixed valve positions that yield desired output values and

(2) simulation functions that predict the response of the mixer to variations in the properties of the LH₂ and GH₂ and manual- or feedback-control variations in valve positions. The GUI enables scheduling of a sequence of operations that includes switching from manual to feedback control when a certain event occurs.

This program was written by Fernando Figueroa of Stennis Space Center, Hanz Richter of the National Research Council, and Enrique Barbieri and Jamie Granger Austin of Tulane University.

Inquiries concerning rights for the commercial use of this invention should be addressed to the Intellectual Property Manager, Stennis Space Center, (228) 688-1929. Refer to SSC-00213.

Control Program for an Optical-Calibration Robot

A computer program provides semiautomatic control of a moveable robot used to perform optical calibration of video-camera-based optoelectronic sensor systems that will be used to guide automated rendezvous maneuvers of spacecraft. The function of the robot is to move a target and hold it at specified positions. With the help of limit switches, the software first centers or finds the target. Then the target is moved to a starting position. Thereafter, with the help of an intuitive graphical user interface, an operator types in coordinates of specified positions, and the software responds by commanding the robot to move the target to the positions. The software has capabilities for correcting errors and for recording data from the guidance-sensor system being calibrated. The software can also command that the target be moved in a predetermined sequence of motions between specified positions and can be run in an advanced control mode in which, among other things, the target can be moved beyond the limits set by the limit switches.

This program was written by Albert (Nick) Johnston of Marshall Space Flight Center. For further information, contact Sammy Nabors, MSFC Commercialization Assistance Lead, at sammy.a.nabors@nasa.gov. MFS-31925-1

SQL-RAMS

SQL-RAMS (where "SQL" signifies Structured Query Language and "RAMS" signifies Rocketdyne Automated Management System) is a succes-

sor to the legacy version of RAMS — a computer program used to manage all work, nonconformance, corrective action, and configuration management on rocket engines and ground support equipment at Stennis Space Center. The legacy version resided in the FileMaker Pro software system and was constructed in modules that could act as standalone programs. There was little or no integration among modules. Because of limitations on file-management capabilities in FileMaker Pro, and because of difficulty of integration of FileMaker Pro with other software systems for exchange of data using such industry standards as SQL, the legacy version of RAMS proved to be limited, and working to circumvent its limitations too time-consuming. In contrast, SQL-RAMS is an integrated SQL-server-based program that supports all data-exchange software industry standards. Whereas in the legacy version, it was necessary to access individual modules to gain insight into a particular work-status document, SQL-RAMS provides access through a single-screen presentation of core modules. In addition, SQL-RAMS enables rapid and efficient filtering of displayed statuses by predefined categories and test numbers. SQL-RAMS is rich in functionality and encompasses significant improvements over the legacy system. It provides users the ability to perform many tasks, which in the past required administrator intervention. Additionally, many of the design limitations have been corrected, allowing for a robust application that is user centric.

This program was written by Victor O. Alfaro and Nancy J. Casey of The Boeing Co. for Stennis Space Center.

Inquiries concerning rights for the commercial use of this invention should be addressed to the Intellectual Property Manager, Stennis Space Center, (228) 688-1929. Refer to SSC-00207.

Distributing Data From Desktop to Hand-Held Computers

A system of server and client software formats and redistributes data from commercially available desktop to commercially available hand-held computers via both wired and wireless networks. This software is an inexpensive means of enabling engineers and technicians to gain access to current sensor data while working in locations in which such data would otherwise be inaccessible. The sensor data are first gathered by a data-acquisition server computer, then transmitted via a wired network to a data-distribution computer that executes the server portion of the present software. Data in all sensor channels — both raw sensor outputs in millivolt units and results of conversion to engineering units — are made available for distribution. Selected subsets of the data are transmitted to each hand-held computer via the wired and then a wireless network. The selection of the subsets and the choice of the sequences and formats for displaying the data is made by means of a user interface generated by the client portion of the software. The data displayed on the screens of hand-held units can be updated at rates from 1 to somewhat more than 10 times per second.

This program was written by Jason L. Elmore of Marshall Space Flight Center. For further information, contact Sammy Nabors, MSFC Commercialization Assistance Lead, at sammy.a.nabors@nasa.gov. MFS-32017-1

Best-Fit Conic Approximation of Spacecraft Trajectory

A computer program calculates a best conic fit of a given spacecraft trajectory. Spacecraft trajectories are often propagated as conics onboard. The conic-section parameters as a result of the best-conic-fit are uplinked to computers aboard the spacecraft for use in updating predictions of the spacecraft trajectory for operational purposes. In the initial application for which this program was written, there is a requirement to fit a single conic section (necessitated by onboard memory constraints) accurate within 200 microradians to a sequence of positions measured over a 4.7-hour interval. The present program supplants a prior one that could not cover the interval with fewer than four successive conic sections. The present program is based on formulating the best-fit conic problem as a parameter-optimization problem and solving the problem numerically, on the ground, by use of a modified steepest-descent algorithm. For the purpose of this algorithm, optimization is defined as minimization of the maximum directional propagation error across the fit interval. In the specific initial application, the program generates a single 4.7-hour conic, the directional propagation of which is accurate to within 34 microradians easily exceeding the mission constraints by a wide margin.

This program was written by Gurkopal Singh of Caltech for NASA's Jet Propulsion Laboratory. Further information is contained in a TSP (see page 1).

This software is available for commercial licensing. Please contact Karina Edmonds of the California Institute of Technology at (818) 393-2827. Refer to NPO-40622.



Improved Charge-Transfer Fluorescent Dyes

These dyes are expected to be useful as molecular probes in diverse applications.

John H. Glenn Research Center, Cleveland, Ohio

Improved charge-transfer fluorescent dyes have been developed for use as molecular probes. These dyes are based on benzofuran nuclei with attached phenyl groups substituted with, variously, electron donors, electron acceptors, or combinations of donors and acceptors. Optionally, these dyes could be incorporated as parts of polymer backbones or as pendant groups or attached to certain surfaces via self-assembly-based methods.

These dyes exhibit high fluorescence quantum yields — ranging from 0.2 to 0.98, depending upon solvents and chemical structures. The wavelengths, quantum yields, intensities, and lifetimes of the fluorescence emitted by these dyes vary with (and, hence, can be used as indicators of) the polarities of solvents in which they are dissolved: In solvents of increasing polarity, fluorescence spectra shift to longer wavelengths, fluorescence quantum yields decrease, and fluorescence lifetimes increase. The wavelengths, quantum yields, intensities, and lifetimes are also

expected to be sensitive to viscosities and/or glass-transition temperatures.

Some chemical species — especially amines, amino acids, and metal ions — quench the fluorescence of these dyes, with consequent reductions in intensities, quantum yields, and lifetimes. As a result, the dyes can be used to detect these species.

Another useful characteristic of these dyes is a capability for both two-photon and one-photon absorption. Typically, these dyes absorb single photons in the ultraviolet region of the spectrum (wavelengths < 400 nm) and emit photons in the long-wavelength ultraviolet, visible, and, when dissolved in some solvents, near-infrared regions. In addition, these dyes can be excited by two-photon absorption at near-infrared wavelengths (600 to 800 nm) to produce fluorescence spectra identical to those obtained in response to excitation by single photons at half the corresponding wavelengths (300 to 400 nm).

While many prior fluorescent dyes exhibit high quantum yields, solvent-polar-

ity-dependent fluorescence behavior, susceptibility to quenching by certain chemical species, and/or two-photon fluorescence, none of them has the combination of all of these attributes. Because the present dyes do have all of these attributes, they have potential utility as molecular probes in a variety of applications. Examples include (1) monitoring curing and deterioration of polymers; (2) monitoring protein expression; (3) high-throughput screening of drugs; (4) monitoring such chemical species as glucose, amines, amino acids, and metal ions; and (5) photodynamic therapy of cancers and other diseases.

This work was done by Michael Meador of Glenn Research Center.

Inquiries concerning rights for the commercial use of this invention should be addressed to NASA Glenn Research Center, Innovative Partnerships Office, Attn: Steve Fedor, Mail Stop 4-8, 21000 Brookpark Road, Cleveland, Ohio 44135. Refer to LEW-17466-1.



✚ Stability-Augmentation Devices for Miniature Aircraft

Passive mechanical devices help miniature aircraft fly in adverse weather.

Langley Research Center, Hampton, Virginia

Non-aerodynamic mechanical devices are under consideration as means to augment the stability of miniature autonomous and remotely controlled aircraft. Such aircraft can be used for diverse purposes, including military reconnaissance, radio communications, and safety-related monitoring of wide areas. The need for stability-augmentation devices arises because adverse meteorological conditions generally affect smaller aircraft more strongly than they affect larger aircraft: Miniature aircraft often become uncontrollable under conditions that would not be considered severe enough

to warrant grounding of larger aircraft. The need for the stability-augmentation devices to be non-aerodynamic arises because there is no known way to create controlled aerodynamic forces sufficient to counteract the uncontrollable meteorological forces on miniature aircraft.

A stability-augmentation device of the type under consideration includes a mass pod (a counterweight) at the outer end of a telescoping shaft, plus associated equipment to support the operation of the aircraft. The telescoping shaft and mass pod are stowed in the rear of the aircraft. When deployed, they extend below the aircraft.

Optionally, an antenna for radio communication can be integrated into the shaft.

At the time of writing this article, the deployment of the telescoping shaft and mass pod was characterized as passive and automatic, but information about the deployment mechanism(s) was not available. The feasibility of this stability-augmentation concept was demonstrated in flights of hand-launched prototype aircraft.

This work was done by Richard M. Wood of Langley Research Center. For further information, contact the Intellectual Property Team at (757) 864-3521.

LAR-16456-1

✚ Tool Measures Depths of Defects on a Case Tang Joint

Precise measurements can be made consistently.

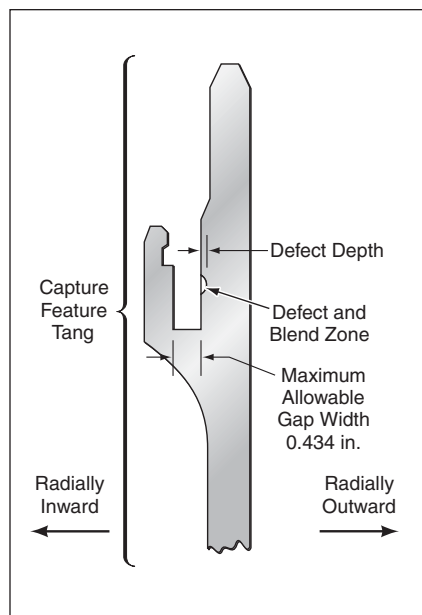
Marshall Space Flight Center, Alabama

A special-purpose tool has been developed for measuring the depths of defects on an O-ring seal surface. The surface lies in a specially shaped ringlike fitting, called a "capture feature tang," located on an end of a cylindrical segment of a case that contains a solid-fuel booster-rocket motor for launching a space shuttle. The capture feature tang is a part of a tang-and-clevis, O-ring joint between the case segment and a similar, adjacent cylindrical case segment. When the segments are joined, the tang makes an interference fit with the clevis and squeezes the O-ring at the side of the gap.

The critical surface in question is an O-ring sealing surface. The defects on this surface can include pits and gouges that must be mitigated by grinding their edges to make them blend smoothly into the surrounding undamaged surface. Measurement of the depths of these defects (see figure) is necessary to ensure against grinding away so much material that the local width of the gap would exceed the maximum allowable value for adequate O-ring squeeze for sealing.

The tool includes four index bearings that ride circumferentially along the interference-fit surface (the inner gap sur-

faces), plus two additional index bearings that ride along the tip of the capture feature. The four-bearing indexing design enables the tool to ride over interference-fit, fretting defects without ad-



The **Depth of a Defect** on the sealing surface of the capture feature tang is what one seeks to measure.

verse effect on the accuracy of measurements. The tool is secured to the case joint by use of two pincher bearings, which ride on the inner-diameter surface of the capture feature. The pincher bearings are connected to spring-loaded handles that apply a radial clamping force. The tool is attached to the joint by squeezing the spring-loaded handles, lowering the device in position, then releasing the handles.

The base of the tool contains a battery compartment and a miniature krypton inspection light. The light is essential for visual inspections inside the gap.

The tool includes a measurement probe on a slide mechanism that enables motion of the probe along the cylindrical axis. There is also an adjustment mechanism for alignment of the slide mechanism with the datum plane established by the four index bearings. The slide is actuated by turning a thumb wheel connected to a spur-gear shaft that, in turn, drives a rack gear, which is mounted on a housing that is part of the probe.

The probe housing, machined from piece of aluminum, contains a dial indicator, a rocker arm, and an engagement-cable release mechanism. The

dial indicator includes a plunger oriented perpendicularly to its bezel. The plunger is spring-loaded and is positioned to push against one end of the rocker arm. The other end of the rocker arm extends into the gap down to the sealing surface of interest, and is fitted with a sharpened contact tip for access to the deepest portions of pit defects. To prevent inadvertent scratching of the sealing surface by the contact tip during circumferential or longitudinal motion of the tool, a spring mechanism

keeps the arm retracted except when a technician actuates the cable-release mechanism to press the tip into contact with the surface.

The tool includes a longitudinal-position dial indicator, which, as its name suggests, shows the longitudinal position of the contact tip of the measurement probe. The spring-loaded plunger of this indicator rests against a bar on the slide mechanism.

The tool is accompanied by a calibration block in the form of a precisely ma-

chined sector simulating a nominal capture feature tang. For storage and transport, the tool is indexed onto the block, then the tool-and-block assembly is placed in a lightweight carrying case with a transparent top.

*This work was done by M. Bryan Ream, Ronald B. Montgomery, Brent A. Mecham, and Burns W. Keirstead of Thiokol Corp. for **Marshall Space Flight Center**. For further information, contact the company at deborah_ledbetter@atk.com. MFS-31398*

Two Heat-Transfer Improvements for Gas Liquefiers

Medical oxygen liquefiers could operate more efficiently.

Lyndon B. Johnson Space Center, Houston, Texas

Two improvements in heat-transfer design have been investigated with a view toward increasing the efficiency of refrigerators used to liquefy gases. The improvements could contribute to the development of relatively inexpensive, portable oxygen liquefiers for medical use.

A description of the heat-transfer problem in a pulse-tube refrigerator is prerequisite to a meaningful description of the first improvement. In a pulse-tube refrigerator — in particular, one of in-line configuration — heat must be rejected from two locations: an aftercooler (where most of the heat is rejected) and a warm heat exchanger (where a small fraction of the total input power must be rejected as heat). Rejection of heat from the warm heat exchanger can be problematic because this heat exchanger is usually inside a vacuum vessel.

When an acoustic-inertance tube is used to provide a phase shift needed in the pulse-tube cooling cycle, another problem arises: Inasmuch as the acoustic power in the acoustic-inertance tube is dissipated over the entire length of the tube, the gas in the tube must be warmer than the warm heat exchanger in order to reject heat at the warm heat exchanger. This is disadvantageous because the increase in viscosity

with temperature causes an undesired increase in dissipation of acoustic energy and an undesired decrease in the achievable phase shift. Consequently, the overall performance of the pulse-tube refrigerator decreases with increasing temperature in the acoustic-inertance tube.

In the first improvement, the acoustic-inertance tube is made to serve as the warm heat exchanger and to operate in an approximately isothermal condition at a lower temperature, thereby increasing the achievable phase shift and the overall performance of the refrigerator. This is accomplished by placing the acoustic-inertance tube inside another tube and pumping a cooling fluid (e.g., water) in the annular space between the tubes. Another benefit of this improvement is added flexibility of design to locate the warm heat-rejection components outside the vacuum vessel.

The second improvement is the development of a compact radial-flow condenser characterized by a very high heat-transfer coefficient and a small pressure drop. The solid heat-transfer medium in this condenser is a core of aluminum foam with a mean pore diameter of ≈ 100 μm and a very high surface-area/volume ratio. At its radially innermost surface, the

aluminum foam core is in contact with a cold head.

The vapor (e.g., oxygen) that one seeks to condense enters the condenser through a feed tube, then flows into an annular inlet plenum that surrounds the foam. The vapor then flows radially inward through the foam, toward the cold head, condensing along the way as it encounters colder foam. At the inner radius, the condenser, the subcooled liquid enters axial holes that lead out of the condenser.

The narrowness of the pores and the high surface-area/volume ratio of the foam give rise to an extremely high volumetric heat transfer coefficient (of the order of $10^6 \text{W/m}^3\text{K}$); as a result, the condenser volume needed to obtain a given degree of cooling is very small. Another advantage of the high heat-transfer coefficient is that little subcooling is needed to condense the vapor and, therefore, the amount of cooling power is less than would otherwise be needed.

This work was done by Jerry L. Martin of Mesoscopic Devices, LLC for Johnson Space Center. For further information, contact the Johnson Technology Transfer Office at (281) 483-3809. MSC-23021/22

Controlling Force and Depth in Friction Stir Welding

The proportionality between penetration force and penetration depth is exploited.

Marshall Space Flight Center, Alabama

Feedback control of the penetration force applied to a pin tool in friction stir welding has been found to be a robust and reliable means for controlling the depth of penetration of the tool. This discovery has made it possible to simplify depth control and to weld with greater repeatability, even on workpieces with long weld joints.

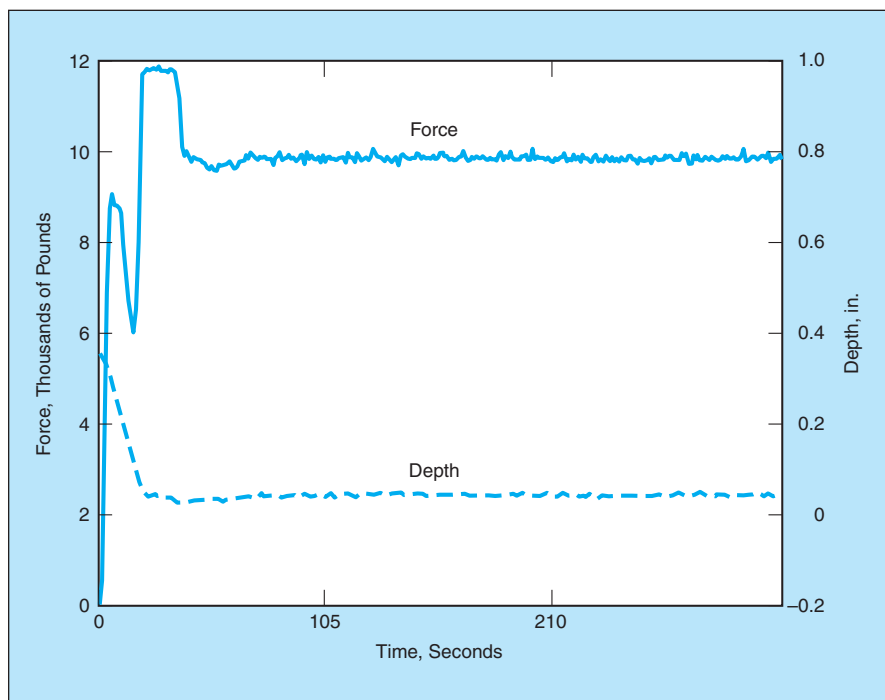
Prior to this discovery, depths of penetration in friction stir welding were controlled by hard-tooled roller assemblies or by depth actuators controlled by feedback from such external sensors as linear variable-differential transformers or

laser-based devices. These means of control are limited:

- A hard-tooled roller assembly confines a pin tool to a preset depth that cannot be changed easily during the welding process.
- A measurement by an external sensor is only an indirect indicative of the depth of penetration, and computations to correlate such a measurement with a depth of penetration are vulnerable to error.

The present force-feedback approach exploits the proportionality between the

depth and the force of penetration. Unlike a depth measurement taken by an external sensor, a force measurement can be direct because it can be taken by a sensor coupled directly to the pin tool. The reading can be processed through a modern electronic servo control system to control an actuator to keep the applied penetration force at the desired level. In comparison with the older depth-control methods described above, this method offers greater sensitivity to plasticizing of the workpiece metal and is less sensitive to process noise, resulting in a more consistent process.



The Force of Penetration Was Maintained within a narrow range, thereby causing the depth of penetration to remain within a narrow range.

In an experiment, a tapered panel was friction stir welded while controlling the force of penetration according to this method. The figure is a plot of measurements taken during the experiment, showing that force was controlled with a variation of 200 lb (890 N), resulting in control of the depth of penetration with a variation of 0.004 in. (0.1 mm).

*This work was done by Glynn Adams, Zachary Loftus, Nathan McCormac, and Richard Venable of Lockheed Martin Corp. for **Marshall Space Flight Center**.*

Title to this invention has been waived under the provisions of the National Aeronautics and Space Act {42 U.S.C. 2457(f)}, to Lockheed Martin Corp. Inquiries concerning licenses for its commercial development should be addressed to:

Lockheed Martin Corp.

Attn. General Counsel

P.O. Box 29304

New Orleans, LA 70189

Telephone No. (504) 257-4786

Refer to MFS-31310, volume and number of this NASA Tech Briefs issue, and the page number.



Spill-Resistant Alkali-Metal-Vapor Dispenser

This dispenser can be used in a gravitational or non-gravitational environment.

NASA's Jet Propulsion Laboratory, Pasadena, California

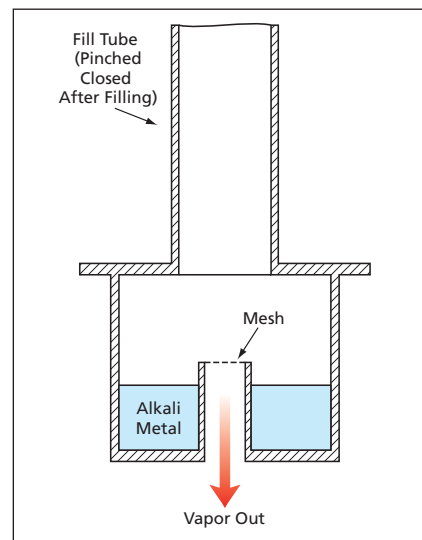
A spill-resistant vessel has been developed for dispensing an alkali-metal vapor. Vapors of alkali metals (most commonly, cesium or rubidium, both of which melt at temperatures slightly above room temperature) are needed for atomic frequency standards, experiments in spectroscopy, and experiments in laser cooling. Although the present spill-resistant alkali-metal dispenser was originally intended for use in the low-gravity environment of outer space, it can also be used in normal Earth gravitation: indeed, its utility as a vapor source was confirmed by use of cesium in a ground apparatus.

The vessel is made of copper. It consists of an assembly of cylinders and flanges, shown in the figure. The uppermost cylinder is a fill tube. Initially, the vessel is evacuated, the alkali metal charge is distilled into the bottom of the

vessel, and then the fill tube is pinched closed to form a vacuum seal.

The innermost cylinder serves as the outlet for the vapor, yet prevents spilling by protruding above the surface of the alkali metal, no matter which way or how far the vessel is tilted. In the event (unlikely in normal Earth gravitation) that any drops of molten alkali metal have been shaken loose by vibration and are floating freely, a mesh cap on top of the inner cylinder prevents the drops from drifting out with the vapor. Liquid containment of the equivalent of 1.2 grams of cesium was confirmed for all orientations with rubbing alcohol in one of the prototypes later used with cesium.

This work was done by William Klipstein of Caltech for NASA's Jet Propulsion Laboratory. Further information is contained in a TSP (see page 1). NPO-40481



Molten Alkali Metal (or any other liquid, for that matter) does not pass through the outlet, no matter which way the vessel is tilted.

A Methodology for Quantifying Certain Design Requirements During the Design Phase

Requirements for safety, reliability, and maintainability are developed and balanced.

John F. Kennedy Space Center, Florida

A methodology for developing and balancing quantitative design requirements for safety, reliability, and maintainability has been proposed. Conceived as the basis of a more rational approach to the design of spacecraft, the methodology would also be applicable to the design of automobiles, washing machines, television receivers, or almost any other commercial product.

Heretofore, it has been common practice to start by determining the requirements for reliability of elements of a spacecraft or other system to ensure a given design life for the system. Next, safety requirements are determined by assessing the total reliability of the system and adding redundant components and subsystems necessary to attain safety goals. As thus described, common practice leaves the maintainability burden to fall to chance; therefore, there is no control of

recurring costs or of the responsiveness of the system. The means that have been used in assessing maintainability have been oriented toward determining the logistical sparing of components so that the components are available when needed.

The process established for developing and balancing quantitative requirements for safety (*S*), reliability (*R*), and maintainability (*M*) derives and integrates NASA's top-level safety requirements and the controls needed to obtain program key objectives for safety and recurring cost (see figure). Being quantitative, the process conveniently uses common mathematical models. Even though the process is shown as being worked from the top down, it can also be worked from the bottom up.

This process uses three math models: (1) the binomial distribution (greater-than-or-equal-to case), (2) reliability for a

series system, and (3) the Poisson distribution (less-than-or-equal-to case). The zero-fail case for the binomial distribution approximates the commonly known exponential distribution or "constant failure rate" distribution. Either model can be used. The binomial distribution was selected for modeling flexibility because it conveniently addresses both the zero-fail and failure cases. The failure case is typically used for unmanned spacecraft as with missiles.

As the first step of the process, the systems engineering designer begins with three inputs: (1) the desired number of missions the program is planning (*n*); (2) the minimum number of successful missions for duration of the program (*x*); and (3) the assurance (*A*) of obtaining *x* or more successes out of the *n* missions. In risk terms, $1 - A$ is the probability or likeli-

hood of not obtaining x or more successes out of n number of attempts or not obtaining the desired level of safety and reliability over the life of the system's program. When these three inputs are used in the binomial distribution, the minimum mission reliability (P_s) is calculated. At this point of

the process, NASA's top-level safety requirement has been established.

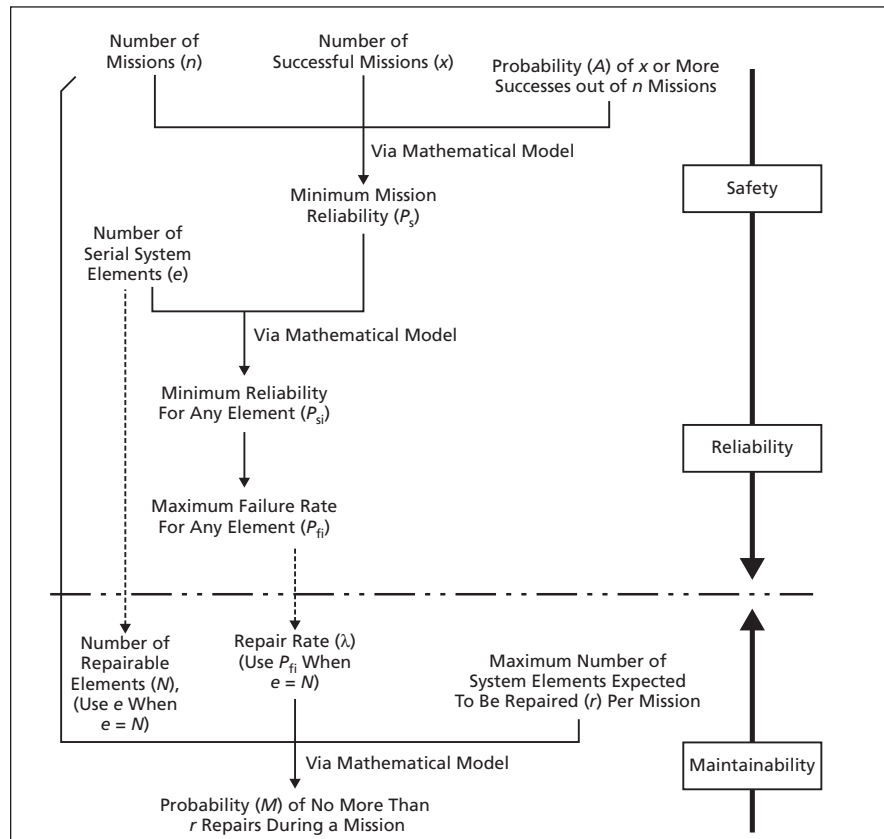
The second step uses the minimum mission reliability (P_s) and an estimate of the number of serial line replaceable unit (LRU) elements (e) as inputs into the formula for reliability of a se-

ries system to calculate minimum element reliability (P_{si}). Maximum element failure rate (P_{fi}) is equal to $1 - P_{si}$. Without considering the maintainability burden, which has a very large influence on recurring cost including the system's acquisition (fleet) size, the process at this point has established the safety and reliability requirements for the program.

The last step addresses the maintainability parameter, the parameter that provides a control for recurring costs resulting from maintenance and repair. Similar to assurance or program reliability (A), program maintainability (M) is a probability. The probability M is determined by the Poisson distribution and uses the following inputs: (1) the number of missions (n), (2) the number of elements (N , where $e \leq N$), (3) the LRU failure rate (P_{fi} or λ , where $\lambda \leq P_{fi}$), and (4) the maximum number of LRU repairs (r). Technically, M is the probability of no more than r number of repairs occurring at a particular mission using e number of LRUs with an average failure rate of P_{fi} or λ .

To achieve the desired results in both M and the desired A , adjustments in e , P_{fi} , N , and λ must be made. These values become the enabling requirements to balance and achieve the desired key objectives of the program.

This work was done by Timothy Adams and Russel Rhodes of Kennedy Space Center. For further information, contact Timothy Adams at (321) 867-2267. KSC-12567



The Process Described in the Text can be run from the top down or from the bottom up as represented in this diagram.

Measuring Two Key Parameters of H3 Color Centers in Diamond

These parameters are needed for the further development of diamond lasers.

NASA's Jet Propulsion Laboratory, Pasadena, California

A method of measuring two key parameters of H3 color centers in diamond has been created as part of a continuing effort to develop tunable, continuous-wave, visible lasers that would utilize diamond as the lasing medium. (An H3 color center in a diamond crystal lattice comprises two nitrogen atoms substituted for two carbon atoms bonded to a third carbon atom. H3 color centers can be induced artificially; they also occur naturally. If present in sufficient density, they impart a yellow hue.) The method may also be applicable to the corresponding parameters of other candidate lasing

media. One of the parameters is the number density of color centers, which is needed for designing an efficient laser. The other parameter is an optical-absorption cross section, which, as explained below, is needed for determining the number density.

The present method represents an improvement over prior methods in which optical-absorption measurements have been used to determine absorption cross sections or number densities. Heretofore, in order to determine a number density from such measurements, it has been necessary to know

the applicable absorption cross section; alternatively, to determine the absorption cross section from such measurements, it has been necessary to know the number density. If, as in this case, both the number density and the absorption cross section are initially unknown, then it is impossible to determine either parameter in the absence of additional information.

In the present method, the needed additional information is extracted from the saturation characteristics of the bulk material: As a laser gain medium (in this case, diamond) absorbs

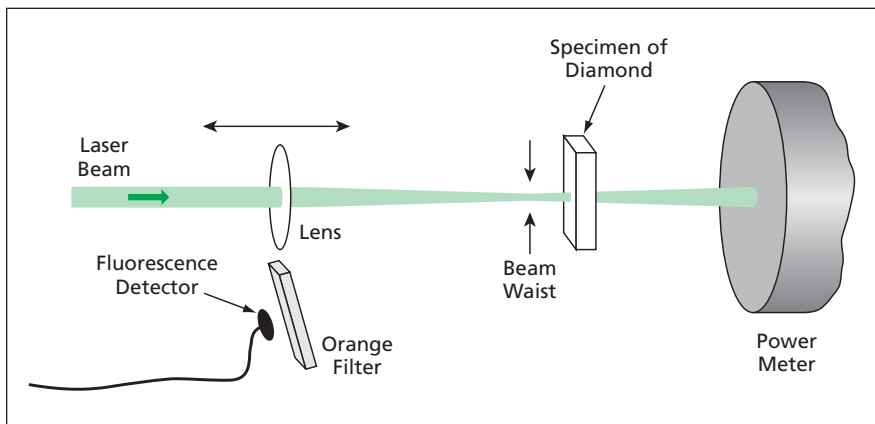


Figure 1. The **Power of a Transmitted Laser Beam** and the level of fluorescence excited by the laser beam are measured at various positions of the beam waist relative to the specimen.

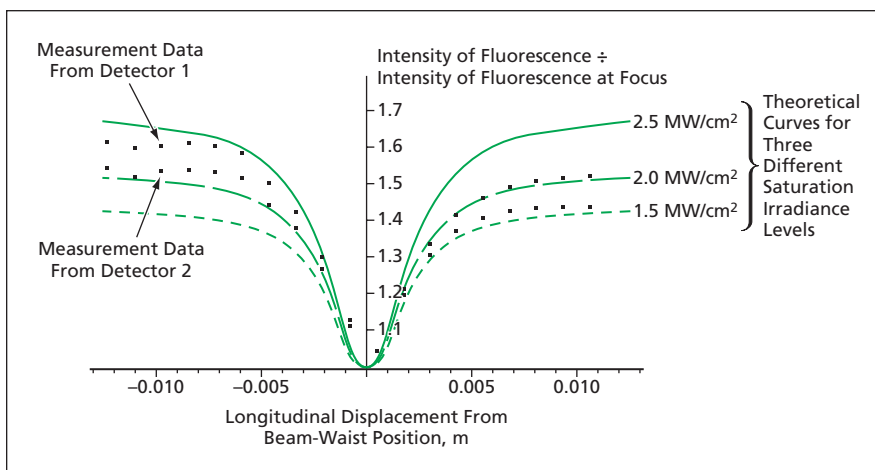


Figure 2. These **Plots of Relative Fluorescence Intensity** versus longitudinal displacement of a diamond specimen from the beam-waist position are typical of the analysis performed in the method described in the text. In this case, the theoretical curve that best fits the readings of two fluorescence detectors represents $I_{\text{sat}} \approx 2 \text{ MW/cm}^2$.

more power from a pump light beam, it begins to absorb a smaller fraction of the incident power. The intensity level at which this saturation effect is observed depends on the atomic-absorption cross section of the material (in this case, the absorption cross section per H3 color center), but not on the number density of color centers. Thus, by measuring the saturation characteristics of the material, the absorption cross section per color center can be determined unambiguously, without knowledge of

the number density. Once the absorption cross section is known, the number density of color centers can be determined, in the conventional manner, from measurements of absorption in the bulk material at intensity below the saturation level.

More specifically, the method is based largely on the following principles:

- The absorption cross section (σ) of a single color center can be obtained from a set of measurements of the absorption saturation irradiance (I_{sat})

and the decay time (τ) of the fluorescence excited by the absorption. For this purpose, I_{sat} can be identified as the level of the probe-beam irradiance above which fluorescence decreases and the fraction of incident probe light transmitted through the specimen increases. The absorption cross section can then be calculated by use of the equation

$$\sigma = hc/\lambda_p I_{\text{sat}} \tau,$$

where h is Planck's constant, c is the speed of light, and λ_p is the wavelength of the monochromatic light used to probe the specimen.

- Once σ is known, the number density (N) of color centers can be obtained from a measurement of transmission (under a non-saturating condition) of a collimated beam of monochromatic light through a specimen of thickness l , by use of the equation

$$N = [\ln(I_0/I)]/\sigma l$$

where I_0 is the irradiance of the beam incident on the specimen and I is the irradiance of the light emerging from the specimen.

The laboratory apparatus for the saturation measurements (see Figure 1) includes a laser that generates a precisely characterized beam and a mechanism for translating the focus (more precisely, the beam waist) through the specimen. By moving the beam waist through the specimen, one can easily vary the irradiance over a wide range. To obtain the value of σ , the fluorescence and transmission measurement data thus obtained at a succession of beam-waist positions (and, hence, at a succession of known irradiance values) are plotted and fitted to theoretical curves of transmission and fluorescence as functions of irradiance (see Figure 2).

This work was done by W. Thomas Roberts of Caltech for NASA's Jet Propulsion Laboratory. Further information is contained in a TSP (see page 1). NPO-30796



Improved Compression of Wavelet-Transformed Images

Code parameters are selected adaptively to achieve high compression performance.

NASA's Jet Propulsion Laboratory, Pasadena, California

A recently developed data-compression method is an adaptive technique for coding quantized wavelet-transformed data, nominally as part of a complete image-data compressor. Unlike some other approaches, this method admits a simple implementation and does not rely on the use of large code tables.

A common data compression approach, particularly for images, is to perform a wavelet transform on the input data, and then losslessly compress a quantized version of the wavelet-transformed data. Under this compression approach, it is common for the quantized data to include long sequences, or "runs," of zeros.

The new coding method uses prefix-free codes for the nonnegative integers as part of an adaptive algorithm for compressing the quantized wavelet-transformed data by run-length coding. In the form of run-length coding used here, the data sequence to be encoded is parsed into strings consisting of some number (possibly 0) of zeros, followed by a nonzero value. The nonzero value and the length of the run of zeros are encoded. For a data stream that contains a sufficiently high frequency of zeros,

this method is known to be more effective than using a single variable length code to encode each symbol. The specific prefix-free codes used are from two classes of variable-length codes: a class known as Golomb codes, and a class known as exponential-Golomb codes. The codes within each class are indexed by a single integer parameter.

The present method uses exponential-Golomb codes for the lengths of the runs of zeros, and Golomb codes for the nonzero values. The code parameters within each code class are determined adaptively on the fly as compression proceeds, on the basis of statistics from previously encoded values. In particular, a simple adaptive method has been devised to select the parameter identifying the particular exponential-Golomb code to use. The method tracks the average number of bits used to encode recent runlengths, and takes the difference between this average length and the code parameter. When this difference falls outside a fixed range, the code parameter is updated (increased or decreased). The Golomb code parameter is selected based on the average magnitude of recently encoded nonzero samples.

The coding method requires no floating-point operations, and more readily adapts to local statistics than other methods. The method can also accommodate arbitrarily large input values and arbitrarily long runs of zeros. In practice, this means that changes in the dynamic range or size of the input data set would not require a change to the compressor.

The algorithm has been tested in computational experiments on test images. A comparison with a previously developed algorithm that uses large code tables (generated via Huffman coding on training data) suggests that the data-compression effectiveness of the present algorithm is comparable to the best performance achievable by the previously developed algorithm.

This work was done by Aaron Kiely and Matthew Klimesh of Caltech for NASA's Jet Propulsion Laboratory. Further information is contained in a TSP (see page 1).

The software used in this innovation is available for commercial licensing. Please contact Karina Edmonds of the California Institute of Technology at (818) 393-2827. Refer to NPO-40490.

NASA Interactive Forms Type Interface — NIFTI

A flexible database query, update, modify, and delete tool provides an easy interface to Oracle forms.

Lyndon B. Johnson Space Center, Houston, Texas

A flexible database query, update, modify, and delete tool was developed that provides an easy interface to Oracle forms. This tool — the NASA interactive forms type interface, or NIFTI — features on-the-fly forms creation, forms sharing among users, the capability to query the database from user-entered criteria on forms, traversal of query results, an ability to generate tab-delimited reports, viewing and downloading of reports to the user's workstation, and a hypertext-based help system. NIFTI is a very powerful *ad hoc* query tool that was developed using C++,

X-Windows by a Motif application framework. A unique tool, NIFTI's capabilities appear in no other known commercial-off-the-shelf (COTS) tool, because NIFTI, which can be launched from the user's desktop, is a simple yet very powerful tool with a highly intuitive, easy-to-use graphical user interface (GUI) that will expedite the creation of database query/update forms. NIFTI, therefore, can be used in NASA's International Space Station (ISS) as well as within government and industry — indeed by all users of the widely disseminated Oracle base. And it will provide sig-

nificant cost savings in the areas of user training and scalability while advancing the art over current COTS browsers.

No COTS browser performs all the functions NIFTI does, and NIFTI is easier to use. NIFTI's cost savings are very significant considering the very large database with which it is used and the large user community with varying data requirements it will support. Its ease of use means that personnel unfamiliar with databases (e.g., managers, supervisors, clerks, and others) can develop their own personal reports. For NASA, a tool such

as NIFTI was needed to query, update, modify, and make deletions within the ISS vehicle master database (VMDB), a repository of engineering data that includes an indented parts list and associated resource data (power, thermal, volume, weight, and the like). Since the VMDB is used both as a collection point for data and as a common repository for engineering, integration, and operations teams, a tool such as NIFTI had to be designed that could expedite the creation of database query/update forms which could then be shared among users.

The present state of the art with COTS browsers means a user must have completed a form to access data in the VMDB. This means a user brings his/her need to the attention of management. The management then brings it to the attention of vehicle data management. The importance of data access is measured against other competing needs for database access, and the required access is eventually deemed sufficiently important to allocate requirements for the VMDB team. This requirement is scheduled for satisfaction at some future release of the VMDB and is assigned to a VMDB team developer. The developer meets with the requester to

hammer out requirements for the form. The form is then implemented with Oracle and is captured within the software configuration management system for the VMDB. There the software will likely exist and continue to be maintained for at least the next decade. If the user requires any changes to the form afterwards, the lengthy process detailed above must be repeated.

NIFTI truncates this process. With NIFTI, a user selects the table he/she wants to access and then selects columns from that table. The field is sized to the user's specifications, and labels and titles are added. A search string is entered on the user's form, including a wildcard, and the user presses the query button. The data needed are now there. If the user is responsible for updating or inserting in the database, he/she corrects the data on the form or enters new data and selects the update or insert button. Since the form has been saved in the database, it has also been saved as part of the database backup; that is, it is not part of the configuration management process. This means that should the user want to add another column or perform a join with

another table, he/she can do this as well. The user can then share created forms with another VMDB user simply by pressing a toggle button and saving. However, should the user not wish to share his/her form, this can be done too by marking the form private. Private forms, which are viewable only by the user, are unlike public forms, which can be viewed by all NIFTI users.

NIFTI is an extremely flexible and reliable tool that can be used in place of Oracle forms. As an X-Windows-based application, NIFTI can run on various platforms. At the time of reporting this information, NIFTI was running on a Sun SPARC workstation at Johnson Space Center.

This work was done by Bobby Jain and Bill Morris of Barrios Technology for Johnson Space Center. For further information, contact:

*Barrios Technology, Inc.
2525 Bay Area Blvd., Suite 300
Houston, TX 77058-1556
Phone: (281) 280-1900
Fax: (281) 280-1901*

Refer to MSC-22914, volume and number of this NASA Tech Briefs issue, and the page number.

Predicting Numbers of Problems in Development of Software

Lyndon B. Johnson Space Center, Houston, Texas

A method has been formulated to enable prediction of the amount of work that remains to be performed in developing flight software for a spacecraft. The basic concept embodied in the method is that of using an idealized curve (specifically, the Weibull function) to interpolate from (1) the numbers of problems discovered thus far to (2) a goal of discovering no new problems after launch (or six months into the future for software already in use in orbit).

The steps of the method can be summarized as follows:

1. Take raw data in the form of problem reports (PRs), including the dates on which they are generated.
2. Remove, from the data collection, PRs that are subsequently withdrawn or to which no response is required.
3. Count the numbers of PRs created in 1-week periods and the running total number of PRs each week.
4. Perform the interpolation by making a

least-squares fit of the Weibull function to (a) the cumulative distribution of PRs gathered thus far and (b) the goal of no more PRs after the currently anticipated launch date. The interpolation and the anticipated launch date are subject to iterative re-estimation.

This work was done by Charles H. Simonds of Lockheed Martin Corp. for Johnson Space Center. For further information, contact the Johnson Innovative Partnerships Office at (281) 483-3809. MSC-23532

Hot-Electron Photon Counters for Detecting Terahertz Photons

A document proposes the development of hot-electron photon counters (HEPCs) for detecting terahertz photons in spaceborne far-infrared astronomical instruments. These would be superconducting-transition-edge devices: they would contain superconducting bridges that would have such low heat capacities that single terahertz photons would cause transient increases in their electron temperatures through the superconducting-transition range, thereby yielding measurable increases in electrical resistance. Single devices or imaging arrays of the devices would be fabricated as submicron-sized bridges made from films of disordered Ti (which has a superconducting-transition temperature of ≈ 0.35 K) between Nb contacts on bulk silicon or sapphire substrates. In operation, these devices would be cooled to a temperature of ≈ 0.3 K. The proposed devices would cost less to fabricate and operate, relative to integrating bolometers of equal sensitivity, which must be operated at a temperature of ≈ 0.1 K.

This work was done by Boris Karasik of Caltech and Andrei Sergeyev of Wayne State University for NASA's Jet Propulsion Laboratory. Further information is contained in a TSP (see page 1). NPO-40660

Magnetic Variations Associated With Solar Flares

A report summarizes an investigation of helioseismic waves and magnetic variations associated with solar flares, involving analysis of data acquired by the Michelson Doppler Imager (MDI) aboard the Solar and Heliocentric Observatory (SOHO) spacecraft, the Yohkoh spacecraft, and the Ramaty High Energy Solar Spectroscopic Imager (RHESSI) spacecraft. Reconstruction of x-ray flare images from RHESSI data and comparison of them with MDI magnetic maps were performed in an attempt to infer the changes in the geometry of the magnetic field. It was established that in most flares observed with MDI, downward propagating shocks were much weaker than was one observed in the July 9, 1996 flare, which caused a strong helioseismic response. It was concluded that most of the observed impulsive variations result from direct impact of high-energy particles. Computer codes were developed for further study of these phenomena.

This work was done by Vahe Petrosian of Stanford University for Goddard Space Flight Center. Further information is contained in a TSP (see page 1). GSC-14694-1

Artificial Intelligence for Controlling Robotic Aircraft

A document consisting mostly of lecture slides presents overviews of artificial-intelligence-based control methods now under development for application to robotic aircraft [called Unmanned Aerial Vehicles (UAVs) in the paper] and spacecraft and to the next generation of flight controllers for piloted aircraft. Following brief introductory remarks, the paper presents background information on intelligent control, including basic characteristics defining intelligent systems and intelligent control and the concept of levels of intelligent control. Next, the paper addresses several concepts in intelligent flight control. The document ends with some concluding remarks, including statements to the effect that (1) intelligent control architectures can guarantee stability of inner control loops and (2) for UAVs, intelligent control provides a robust way to accommodate an outer-loop control architecture for planning and/or related purposes.

This work was done by Kalmanje KrishnaKumar of Ames Research Center. Further information is contained in a TSP (see page 1).

Inquiries concerning rights for the commercial use of this invention should be addressed to the Technology Partnerships Division, Ames Research Center, (650) 604-2954. Refer to ARC-15340-1.

